Identification of Wheel-Rail Contact Condition Using Multi-Kalman Filtering Approach

IMTIAZ HUSSAIN*, ALI ASGHAR MEMON**, AND BHAWANI SHANKAR CHOWDHRY***

RECEIVED ON 06.08.2012 ACCEPTED ON 18.09.2012

ABSTRACT

Condition changes at the rail surface due to the fallen tree leaves and/or other contaminations can cause the low adhesion levels which present a serious challenge for the traction/braking control systems to avoid the problem of wheel slip/slide. This paper presents a multiple model based method for the identification of the adhesion limit to overcome the problem of the wheel slip/slide in poor contact conditions. The proposed scheme is an indirect method that exploits the dynamic properties of the conventional solid axle wheelset in response to changes in contact condition at the wheel-rail interface avoiding difficult and expensive measurement requirements. A nonlinear model of lateral and yaw dynamics of a conventional solid axle wheelset is used for the study. The non-linearity and changes in the interaction with the rail are modelled by using a set of non-linear creep/slip curves. The scheme consists of a bank of Kalman filters based on the linearized wheelset models. Each Kalman filter in the filter bank is optimally tuned to operate in a specific contact condition. Normalized root mean square values from the residual of each filter calculated using time moving windows are assessed to identify the operating condition of the wheelset.

Key Words: **Wheel Rail Contact, Estimation, Kalman Filters, Fuzzy Logic.**

1. INTRODUCTION

The traction and braking performance of the railway vehicle is governed by the contact forces generated at the wheel rail interface. These contact forces are a non-linear function of the creepages and vary substantially when the conditions of the rail surfaces change due to the contaminations. The overall adhesion can therefore becomes very low which results in wheel slip/slide. The wheel Slip/Slide is a highly undesirable phenomenon that causes the mechanical parts to wear down quickly affects the stability and leads to the inconsistent traction performance causing problems in train scheduling.

In order to avoid the wheel slip/slide various different techniques have been used in past [1] presented a conventional technique of controlling the wheel slip based on the measurement of the relative speed between the wheel and the train which was supplemented with the control of the wheel acceleration. Also hybrid anti-slip methods which are also based on the relative speed measurement are proposed [2-3]. These controllers require an accurate measurement of the train and wheel rotational speeds that makes it difficult to obtain the optimal performance. Another method based on disturbance

* Assistant Professor, Department of Electronic Engineering, Mehran University of Engineering & Technology, Jamshoro.
** Assistant Professor, Department of Electrical Engineering, Mehran University of Engineering & Technology, Jamshoro.
*** Meritorious Professor, Department of Electronic Engineering, Mehran University of Engineering & Technology, Jamshoro.

observers are proposed to detect the slip conditions [2,4]. These controllers do not require direct speed measurement rather the adhesion coefficient is estimated by using the information of rotor speed and the torque current but the performances of the anti-slip schemes based on a disturbance observer are to a large extent affected by noises in the system which can be very substantial in the wheel-rail contact environment [5] proposes an indirect technique that exploits the wheelset dynamics to develop wheel slip protection.

The real time information about the maximum adhesion available as a train travels through a track would help to tackle the problem of the wheel slip/slide. The provision of the tractive effort in either traction or braking could then be optimised to make the most out of the wheel-rail contact conditions.

This paper is an extension of an ongoing research that uses the multiple model based estimation approach for the identification of the contact conditions [6-8]. In a previous study, the residual of estimated states were examined to determine the operating condition. In this paper a fuzzy logic based identification method is developed to determine the contact condition.

2. WHEELSET MODELLING

A solid axle railway wheelset (Fig. 1) with both the wheels fixed with the axle is used for this study. Both the wheels have profiled tread with the conicity γ. This coned tread provides a natural feedback (due to the difference in the rolling radius) for the wheelset to adjust itself on the centre position when it is slightly displaced laterally. The motions of the wheelset are governed by the nonlinear creep forces generated at the wheel rail contact patch in the lateral and longitudinal directions. Creep is said to exist when the railway wheels deviate from pure rolling and can be described as the relative motion of wheels to the rails given in Equations (1-3). Delivery of tractive effort in traction and braking is achieved via longitudinal creep.

$$\lambda_{xL} = \frac{r_o\omega_L - v}{v} + \left[\frac{L_g\dot{\psi}}{v} + \frac{\gamma\left(y - y_t\right)}{r_o}\right] \tag{1}$$

$$\lambda_{xR} = \frac{r_o\omega_R - v}{v} - \left[\frac{L_g\dot{\psi}}{v} + \frac{\gamma\left(y - y_t\right)}{r_o}\right] \tag{2}$$

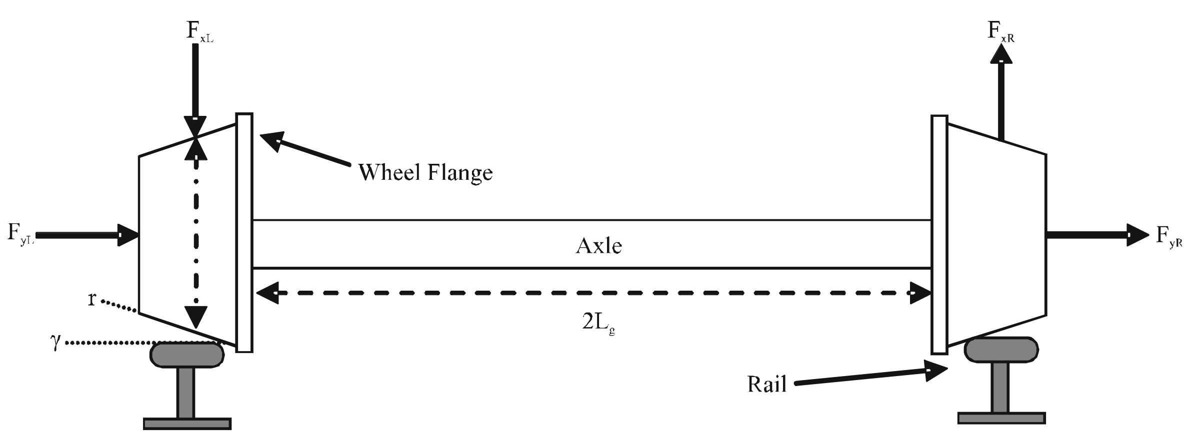

FIG. 1. RAILWAY WHEELSET

$$\lambda_{yL} = \lambda_{yR} = \frac{\dot{y}}{v} - \psi \tag{3}$$

In Equations (1-3) the subscript L,R are used for left and right wheels respectively, x and y are used to indicate the longitudinal and lateral directions, and γ_{xL}, γ_{xR}, γ_{yL} and γ_{yR} are creepages in the longitudinal and lateral directions for left and right wheels. γ_R and γ_L are angular speeds of right and left wheels respectively, γ is yaw angle, y is lateral motion, L_g is the half track gauge, v is forward speed of the vehicle, γ is conicity of wheel and r_o is the radius of wheel when it is at centre position and y_t is disturbance applied by track in lateral direction. The total creep at any point on the creep curve is given by Equations (4-5):

$$\lambda_L = \sqrt{\lambda_{xL}^2 + \lambda_{yL}^2} \tag{4}$$

$$\lambda_R = \sqrt{\lambda_{xR}^2 + \lambda_{yR}^2} \tag{5}$$

2.1 Simplified Model

Only lateral and yaw dynamics are found to be sufficient to identify the track condition [8]. The simplified equations of longitudinal creep for the left and the right wheel are given in Equations (6-7):

$$\lambda_{xL} = \frac{L_g \dot{\psi}}{v} + \frac{\gamma\left(y - y_t\right)}{r_o} \tag{6}$$

$$\lambda_{xR} = -\frac{L_g \dot{\psi}}{v} - \frac{\gamma\left(y - y_t\right)}{r_o} \tag{7}$$

The yaw angle is the result of the difference in the longitudinal creep forces between the two wheels and the lateral dynamics are determined by the total creep force of the two wheels in the lateral direction. The relationship for the lateral and the yaw motions of the railway wheelset are given in Equations (8-9).

$$m_w \ddot{y} = -f_{yR} - f_{yL} + F_c \tag{8}$$

$$I_w \ddot{\psi} = f_{xR} L_g - f_{xL} L_g - k_w \psi \tag{9}$$

Where m_w is the wheelset mass, F_c is the centrifugal component of the force and can be ignored if the wheelset is not running on the curved track, I_w is the yaw moment of inertia and k_w is the yaw stiffness of a spring used to stabilise the wheelset. f_{yL}, f_{yR}, f_{xL} and f_{xR} are the creep forces of left and right wheels in lateral and longitudinal directions.

The creep forces in Equation (8-9) are widely recognised to present the non-linear characteristics as a function of creep as shown in Fig. 2. The creep curve shown in Fig. 2 represent good contact condition is obtained using Polach model [9]. In normal running conditions where the creep is small, the contact forces provide a damping effort to the dynamic modes of a wheelset and are very useful in stabilising those modes. As the creep increases, due to application of tractive effort, the contact forces can operate in the second (or non-linear) region where the rate of change of the creep forces and associated damping effect is much lower. However, when the creep is beyond the point of maximum adhesion (μm) available at the wheel-rail interface and enters the slip or unstable region, the contact forces will then become a destabilising element, which not only cause the well known problem of wheel slip (in traction) or slide (in braking) but also can cause other undesirable mechanical oscillations in the wheelset [6].

3. KALMAN FILTER DESIGN

Kalman filter is a useful tool to estimate the parameters of a linear stochastic process with unknown disturbances, such as the railway wheelset with unknown track disturbance, with some knowledge of the process output and the model. As it works well when the system is linear the nonlinear creep forces are linearized at specific point on the creep curve (λ_o, μ_o) as shown in Equation (10) [7]. The derivative terms represent the slope on the creep curve at the point of linearization which is simplified and represented by g_{11} and g_{12}.

$$
\begin{aligned}
f_{xR} = f_{xRo} &+ \left.\frac{\partial f_{xR}}{\partial \lambda_{xR}}\right|(\lambda_{xRo}, \lambda_{yRo}) \times \Delta\lambda_{xR} \\
&+ \left.\frac{\partial f_{xR}}{\partial \lambda_{yR}}\right|(\lambda_{xRo}, \lambda_{yRo}) \times \Delta\lambda_{yR}
\end{aligned}
\qquad (10)
$$

or

$$f_{xR} = f_{xRo} + g_{11}\Delta\lambda_{xR} + g_{12}\Delta\lambda_{yR} \qquad (11)$$

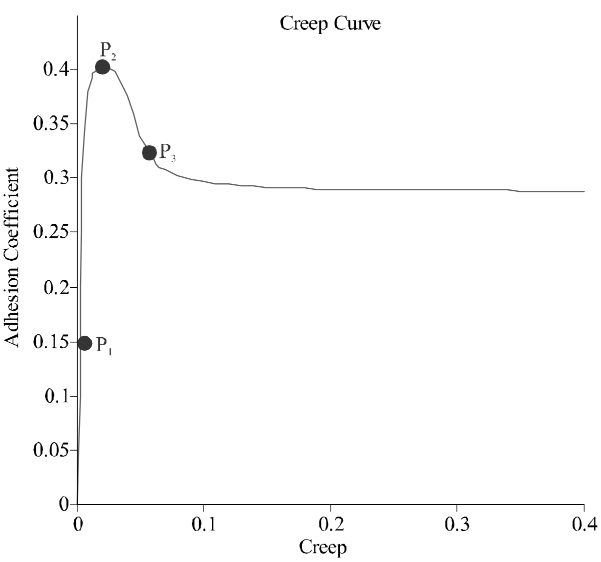

FIG. 2. ADHESION COEFFICIENT VARIATION

All the creep forces are linearized in the similar way and the linearized small signal model of the lateral and yaw dynamics of the railway wheelset is obtained in Equation (12).

$$
\begin{bmatrix} \Delta\dot{y} \\ \Delta\dot{\psi} \\ \Delta\ddot{y} \\ \Delta\ddot{\psi} \end{bmatrix}
=
\begin{bmatrix}
0 & 0 & 1 & 0 \\
0 & 0 & 0 & 1 \\
0 & \dfrac{2g_{22}}{m_w} & -\dfrac{2g_{22}}{vm_w} & 0 \\
-\dfrac{2L_g\gamma g_{11}}{r_o I_w} & -\dfrac{k_w}{I_w} & 0 & -\dfrac{2L_g^2 g_{11}}{vI_w}
\end{bmatrix}
\begin{bmatrix} \Delta y \\ \Delta\psi \\ \Delta\dot{y} \\ \Delta\dot{\psi} \end{bmatrix}
+
\begin{bmatrix} 0 \\ 0 \\ 0 \\ \dfrac{2L_g\gamma g_{11}}{r_o I_w} \end{bmatrix}
\Delta y_t
\qquad (12)
$$

This model is valid only at specific operating point on the creep curve and best estimation results may be obtained when the wheelset is operated in the vicinity of the point where it is linearized. Equation (12) gives us idea how the dynamics of the wheelset are affected when operating point of the wheelset (i.e. g_{11} and g_{22}) is changed. Table 1 summerized the values of parameters used during the simulations. With the change in operating point linearized creep coefficients g_{11} and g_{22} also change, which as a result changes the system dynamics.

TABLE 1. PARAMETER VALUES

Parameter	Description	Value
I_w	Yaw Moment of Inertia of the Wheelset (kgm^2)	700
r_o	Rolling Radius of the Wheels at Centre Position (meters)	0.5
γ_w	Conicity of the Wheel Tread (radians)	0.15
L_g	Track Half Gauge (meters)	0.75
m_w	Mass of the Wheelset (kg)	1250
k_w	Yaw Stiffness (N/rad)	5×10^6
I_R	Right Wheel Moment of Inertia (kgm^2)	68.2
I_R	Right Wheel Moment of Inertia (kgm^2)	133.2

3.1 Kalman Filter Formulation

The wheelset dynamics are excited by the unknown track disturbance. In order to obtain a good estimation results the unknown track disturbance is treated as part of the state vector as shown in the Equation (13), where it is assumed that $\Delta\dot{y}_t = -0.001 + \dot{y}_t$.

$$\frac{d}{dt}\begin{bmatrix}\Delta\psi \\ \Delta\dot{y} \\ \Delta\dot{\psi} \\ \Delta y_t \\ \Delta y-\Delta y_t\end{bmatrix} = \begin{bmatrix} 0 & 0 & 1 & 0 & 0 \\ \frac{2g_{22}}{m_w} & -\frac{2g_{22}}{vm_w} & 0 & 0 & 0 \\ -\frac{k_w}{I_w} & 0 & -\frac{2L_g^2 g_{11}}{vI_w} & 0 & -\frac{2L_g \gamma g_{11}}{r_o I_w} \\ 0 & 0 & 0 & -0.001 & 0 \\ 0 & 1 & 0 & 0 & 0 \end{bmatrix} \begin{bmatrix}\Delta\psi \\ \Delta\dot{y} \\ \Delta\dot{\psi} \\ \Delta y_t \\ \Delta y-\Delta y_t\end{bmatrix} + \begin{bmatrix}0 \\ 0 \\ 0 \\ 1 \\ -1\end{bmatrix}\Delta\dot{y}_t \tag{13}$$

Two sensors (A gyro sensor for the yaw rate measurement and an accelerometer for the lateral acceleration measurement) as indicated in Equation (14) (v is a vector representing noise level of the sensors with the covariance R) appear to be sufficient for the Kalman filter to provide satisfying estimation results.

$$z(t) = \begin{bmatrix} 0 & 0 & 1 & 0 & 0 \\ \frac{2g_{22}}{m_w} & -\frac{2g_{22}}{vm_w} & 0 & 0 & 0 \end{bmatrix} \begin{bmatrix}\Delta\psi \\ \Delta\dot{y} \\ \Delta\dot{\psi} \\ \Delta y_t \\ \Delta y-\Delta y_t\end{bmatrix} + v \tag{14}$$

Fig. 3 shows the multiple Kalman filter based estimators. Each Kalman filter design is based on the small signal model linearized at specific point on the creep curve. The Kalman filters are optimally tuned by selecting optimal value of covariance matrix R.

The complete proposed scheme is shown in the Fig. 4. Only three filters are used here to show the potential of the research. The three chosen operating points are shown in Fig. 2 as P_1 (Linear Region of the Creep Curve), P_2 (Maximum Point of the creep curve where rate of change of creep force is zero) and P_3 (Unstable Region). Filter-1, Filter-2 and Filter-3 are designed to operate at these points respectively. The tuning of filters is done by trial and error method. At any specific operating point filter tuning parameters are varied until the estimation error at that point is lowest. The choice of linearization points is based on the variation of the adhesion coefficient with respect to creep. The creep curve is divided into three segments (i.e. Linear, nonlinear and unstable) therefore one operating point chosen in each segment. Number of Kalman filters can be increased easily to include all possible contact conditions. The normalized values of the residuals of estimated states are then calculated with moving time window of one second (Equation (15)). Normalized values of residuals of lateral acceleration are shown in Figs. 5-7 when the wheelset was operated at P_1, P_2 and P_3 respectively. Error-1, Error-2 and Error-3 are the errors produced by Filter-1, Filter-2 and Filter-3 respectively.

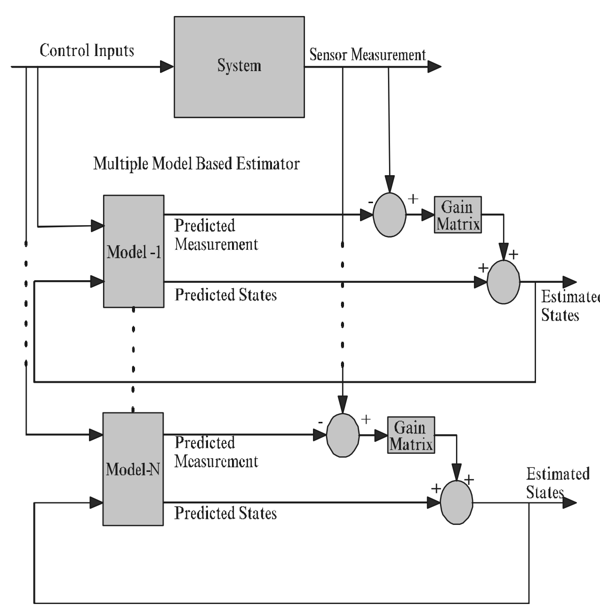

FIG. 3. MULTIPLE MODEL BASED ESTIMATION [8]

$$E_{1-rms} = \frac{\frac{1}{\Delta t}\int_{t-\Delta t}^{t}(E_{1-rms}(t))^2 dt}{\sqrt{\frac{1}{\Delta t}\int_{t-\Delta t}^{t}(E_{1-rms}(t))^2 dt + \frac{1}{\Delta t}\int_{t-\Delta t}^{t}(E_{2-rms}(t))^2 dt + \frac{1}{\Delta t}\int_{t-\Delta t}^{t}(E_{3-rms}(t))^2 dt}} \quad (15)$$

The results show when the wheelset is operated around a point where the any specific filter is optimally tuned to operate the respective filter has minimum error around that point also the amount of error is increased or decreased depending upon how far the wheelset is operating from that point. This provides an excellent opportunity to develop a fuzzy logic based identification system based on these results as shown in Fig. 8.

The normalized values of the residuals are fed to the fuzzy logic system with specific membership function which associates a weighting with each of the input that are processed. The weighting function determines the amount of participation of each input in the

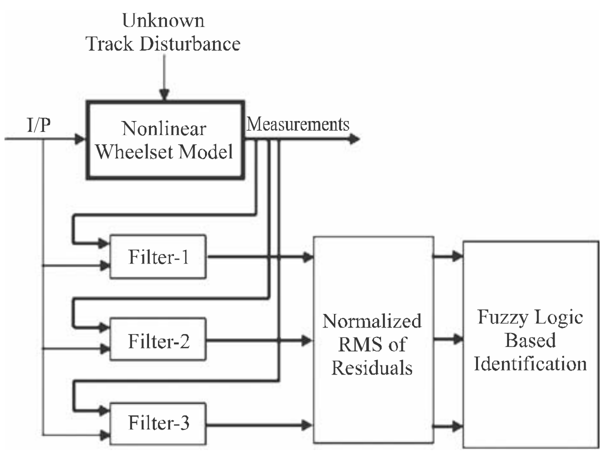

FIG. 4. CONTACT CONDITION IDENTIFICATION SCHEME

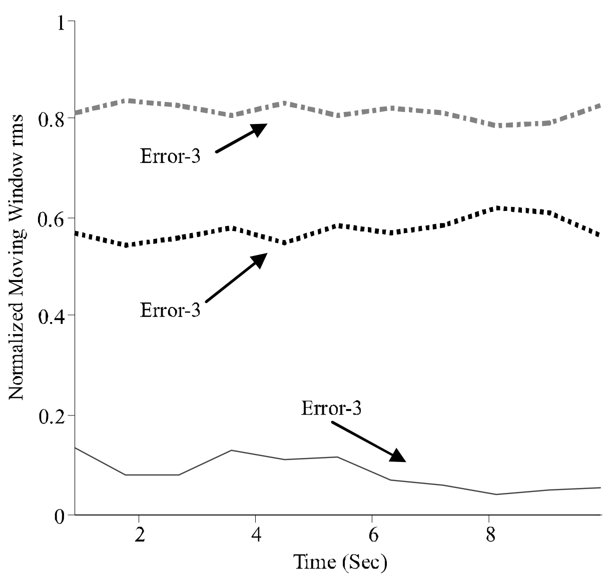

FIG. 5. NORMALIZED RMS OF RESIDUALS AT P_1

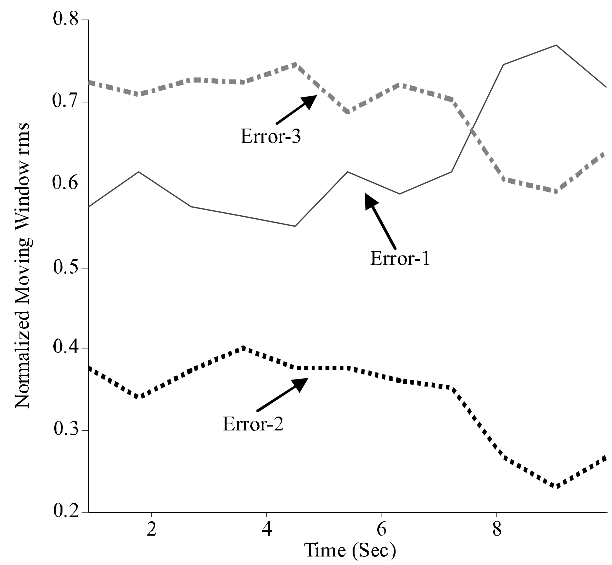

FIG. 6. NORMALIZED RMS OF RESIDUALS AT P_2

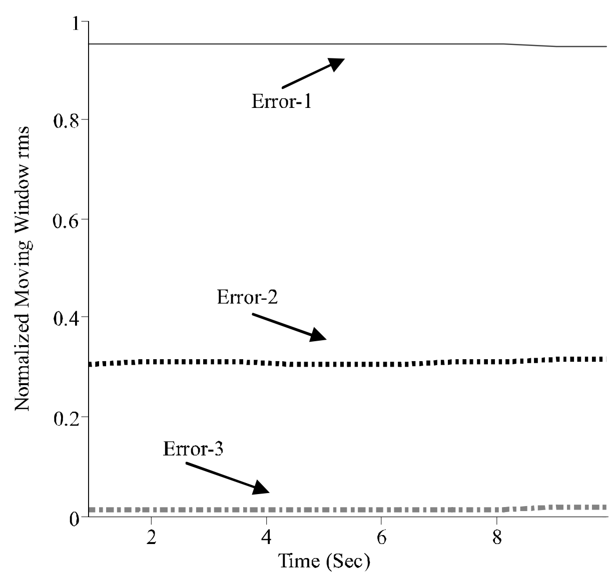

FIG. 7. NORMALIZED RMS OF RESIDUALS AT P_3

producing the output. The rules use the input membership values as weighting factors to determine their influence on the output. Output is produced in terms of the probability of the operating point near to P_1, P_2 and P_3. Fig. 9 is an example out of the system when the wheelset was operated in the vicinity of P_1. The fuzzy output indicates 90% probability of operating point is around P_1. The simulation was carried out at various different operating points and the results showed excellent agreement with the theory.

4. CONCLUSION

The good delivery of the tractive effort in the traction and braking can be achieved through the real time knowledge of the contact condition. This research proposes a novel technique to identify the contact condition by investigating the changes in the dynamic properties of the wheelset as the train travel through the track. The proposed scheme indirectly identifies the contact condition with minimum measurement requirement. The results presented show the satisfactory performance. However, the simulation is carried out using only one creep curve representing good/dry contact condition with small changes in the creep due to application of the tractive torque. Further research is been carried out to validate this model on different creep curves representing low adhesion conditions with large changes in the creep forces.

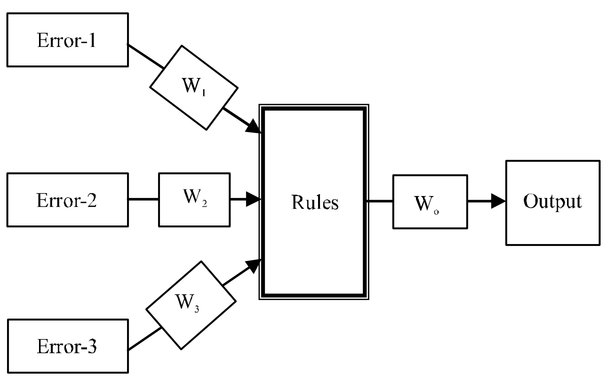

FIG. 8. FUZZY LOGIC BASED IDENTIFICATION SYSTEM

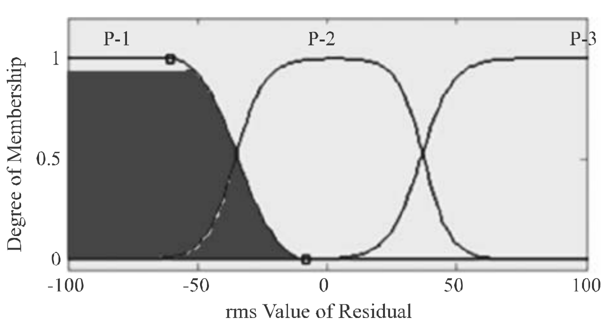

FIG. 9. OUTPUT MEMBERSHIP FUNCTION

ACKNOWLEDGEMENTS

Authors would like to thank the Mehran University of Engineering & Technology, Jamshoro, Pakistan, and University of Salford, UK, for providing the financial support and research facilities for our research work.

REFERENCES

[1] Watanabe, T., and Yamanaka, A., "Optimisation of Readhesion Control of Shinkansen Trains with Wheel-Rail Adhesion", Proceedings of the Power Conversion Conferecne, pp. 47-50, Nagaoka, Japan, 1997.

[2] Choi, H., and Hong, S., "Hybrid Control for Longitudinal Speed and Traction of Vehicles", 28th Annual Conferecne on IEEE Industrial Society, Volume 2, pp. 1675-1680, Suwon, South Korea, 5-8 November, 2002.

[3] Park, D., Moon-Sup, K., Don-Ha, H., Joo-Hoon, L., and Yong-Joo, K., "Hybrid Re-Adhesion Control Method for Traction System of High-Speedrailway", Proceedings of the 5th International Conferecne on Electrical Machines and Systems, pp. 739-742, Korea, 2001.

[4] Kim, W., Kim, Y., Kang, J., and Sul, K., “Electro-Mechanical Re-Adhesion Control Simulator for Inverter-Driven Railway Electric Vehicle", Proceedings of the 34th IEEE Industrial Application Conferecne, Volume 2, pp. 1026-1032, Phoenix AZ, 6th August, 2002.

[5] Mei, T.X., Yu, J., and Wilson, D., "A Mechatronic Approach for Effective Wheel Slip Control in Railway Traction", Proceedings of the Institution of Mechanical Engineers, Journal of Rail and Rapid Transit, Part-F, Volume 223, No. 3, pp. 295-304, 2009.

[6] Mei, T.X., and Hussain, I., "Detection of Wheel-Rail Contact Conditions for Improved Traction Control", Proceedings of 4th International Conference on Railway Traction Systems, Birmingham, UK, 2010.

[7] Hussain, I., Mei, T.X., and Jones, A.H., "Modeling and Estimation of Nonlinear Wheel-Rail Contact Mechanics", Proceedings of Twentieth Intenational Conference on System Engineering, pp. 219-223, Coventry, UK, 2009.

[8] Hussain, I., and Mei, T.X., "Multi Kalman Filtering Approach for Estimation of Wheel-Rail Contact Conditions", Proceedings of the United Kingdom Automatic Control Conferecne, Coventry, UK, 2010.

[9] Polach, O., "Creep Forces in Simulations of Traction Vehicles Running on Adhesion Limit". Wear, Volume 58, No. 1, pp. 992-1000, 2005.